Dielectric-Loaded Plasmonic Switching Elements and Circuits

A. Pitilakis, O. Tsilipakos and E. E. Kriezis

Session: **Waveguide optics modeling**

Outline

- Introduction
  - The DLSPP Waveguide
  - DLSPP-Based Components
  - The Big Picture & Challenges
- Microring-Based Resonant Switching Elements
  - Classic Add-Drop Filter
  - 3D FEM Implementation Details
  - Waveguide Crossing
  - Add-Drop Filter with Perpendicular Access Waveguides
  - Dual-Resonator Add-Drop filter with perpendicular access waveguides
- Longitudinal Switching Elements
  - A Multi-Mode Interference (MMI) Approach
  - 3D BPM Implementation Details
  - Dispersion Studies
  - Theoretical Bounds in Performance
  - Switch Evaluation using BPM
- Conclusions

Outline

- Introduction
  - The DLSPP Waveguide
  - DLSPP-Based Components
  - The Big Picture & Challenges
- Microring-Based Resonant Switching Elements
  - Classic Add-Drop Filter
  - 3D FEM Implementation Details
  - Waveguide Crossing
  - Add-Drop Filter with Perpendicular Access Waveguides
  - Dual-Resonator Add-Drop filter with perpendicular access waveguides
- Longitudinal Switching Elements
  - A Multi-Mode Interference (MMI) Approach
  - 3D BPM Implementation Details
  - Dispersion Studies
  - Theoretical Bounds in Performance
  - Switch Evaluation using BPM
- Conclusions

Outline

- Introduction
  - The DLSPP Waveguide
  - DLSPP-Based Components
  - The Big Picture & Challenges
- Microring-Based Resonant Switching Elements
  - Classic Add-Drop Filter
  - 3D FEM Implementation Details
  - Waveguide Crossing
  - Add-Drop Filter with Perpendicular Access Waveguides
  - Dual-Resonator Add-Drop filter with perpendicular access waveguides
- Longitudinal Switching Elements
  - A Multi-Mode Interference (MMI) Approach
  - 3D BPM Implementation Details
  - Dispersion Studies
  - Theoretical Bounds in Performance
  - Switch Evaluation using BPM
- Conclusions

Outline

- Introduction
  - The DLSPP Waveguide
  - DLSPP-Based Components
  - The Big Picture & Challenges
- Microring-Based Resonant Switching Elements
  - Classic Add-Drop Filter
  - 3D FEM Implementation Details
  - Waveguide Crossing
  - Add-Drop Filter with Perpendicular Access Waveguides
  - Dual-Resonator Add-Drop filter with perpendicular access waveguides
- Longitudinal Switching Elements
  - A Multi-Mode Interference (MMI) Approach
  - 3D BPM Implementation Details
  - Dispersion Studies
  - Theoretical Bounds in Performance
  - Switch Evaluation using BPM
- Conclusions

Introduction: Surface Plasmon Polaritons

Surface Plasmon Polaritons (SPPs):

Electromagnetic surface waves coherently coupled to free electron oscillations.

- Propagate along a metal-dielectric interface.
- Fields decay exponentially away from the interface.
- Exhibit propagation losses due to resistive damping in the metallic film.
- Trade-off between propagation losses and lateral confinement.

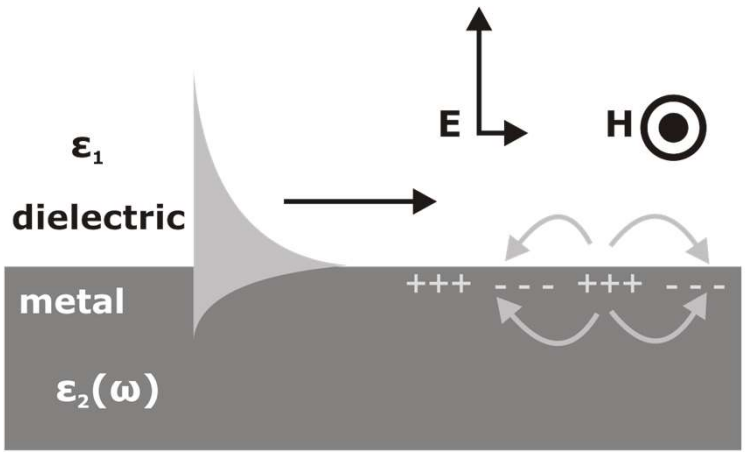

SPP at single metal-dielectric interface:
An elementary plasmonic waveguide.

Introduction: The DLSPP Waveguide

Dielectric-loaded surface plasmon polariton (DLSPP) waveguide:

- ✓ Technologically simple.
- ✓ (2D) Sub-wavelength confinement and strong guiding properties.
- ✓ Relatively low propagation losses (L_{prop} ~ 45 μm for TM_{00} mode).
- ✓ Readily accommodates diverse loadings → Dynamic components.

T. Holmgaard, S.I. Bozhevolnyi, *Phys. Rev. B*, 75, 245405, 2006

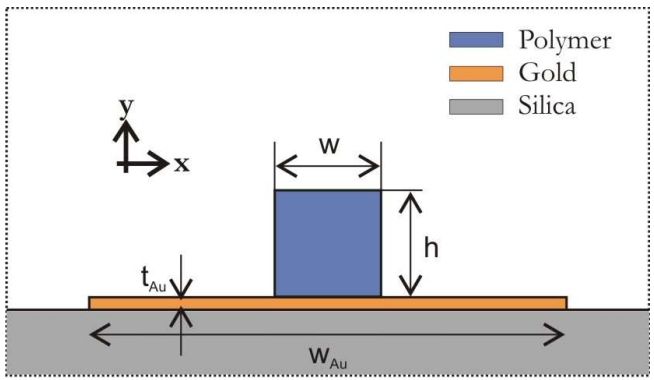

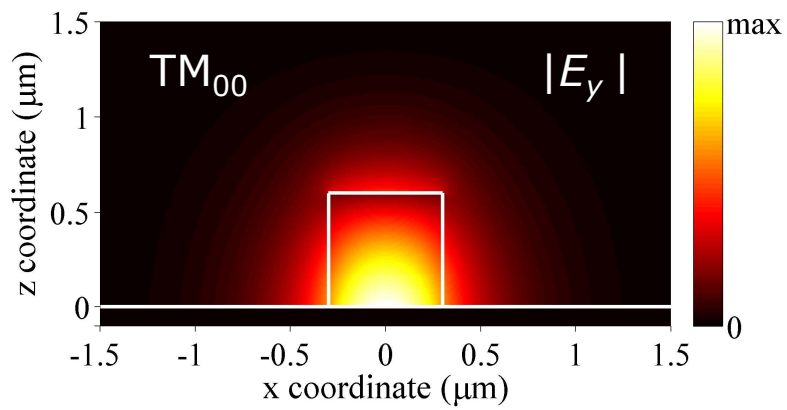

$w \times h$ = 500×600 nm^2 // t_{Au} = 100 nm
n_{pol} ~ 1.5 // $\varepsilon_{r,Au}$ = -132 – j*12.65 @ λ = 1.55 μm

Introduction: DLSPP-Based Components

A broad range of passive components has been studied and experimentally demonstrated, including:

- ✓ Waveguide bends
- ✓ Coupled lines
- ✓ Splitters

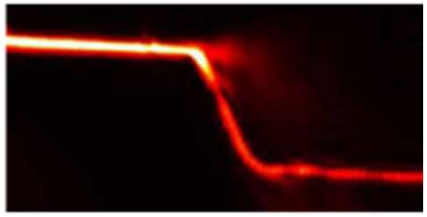

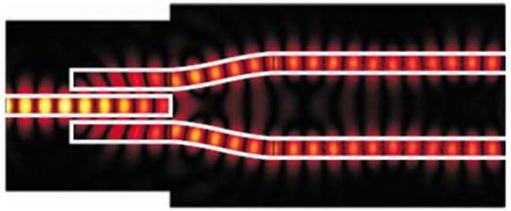

A.V. Krasavin, A.V. Zayats, *Phys. Rev. B*, 78, 045425, 2008
T. Holmgaard, *et al.*, *Opt. Express*, 16, 13586, 2008

- ✓ Bragg reflectors
- ✓ Directional couplers
- ✓ Mach-Zehnder Interferometers

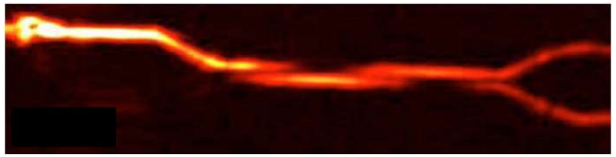

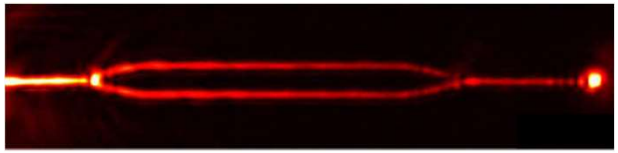

T. Holmgaard, *et al.*, *Appl. Phys. Lett.*, 94, 051111, 2009
Z. Chen, *et al.*, *Opt. Lett.*, 34, 310, 2009

Introduction: DLSPP-Based Components

More recently, interest is focused on wavelength-selective components:

- ✓ Microring & racetrack resonator filters
- ✓ Microdisk resonator filters
- ✓ Add-Drop filters

R. Briggs, *et al.*, *Nano Lett.*, 10, 4851, 2010

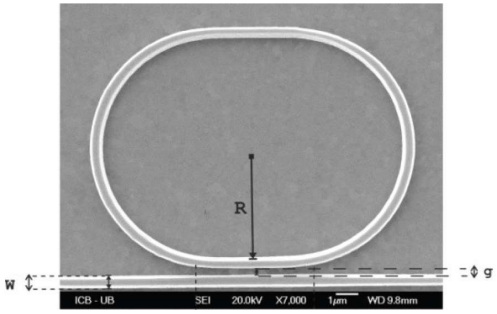

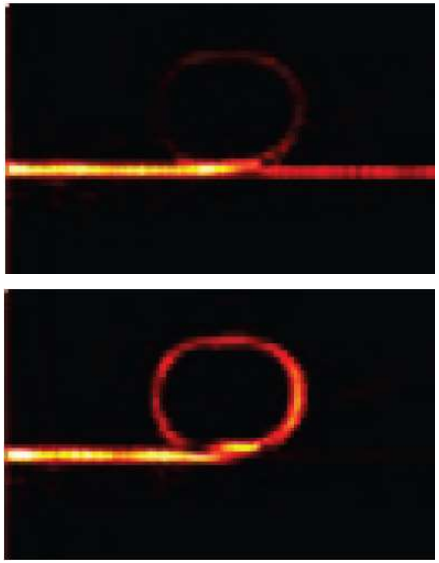

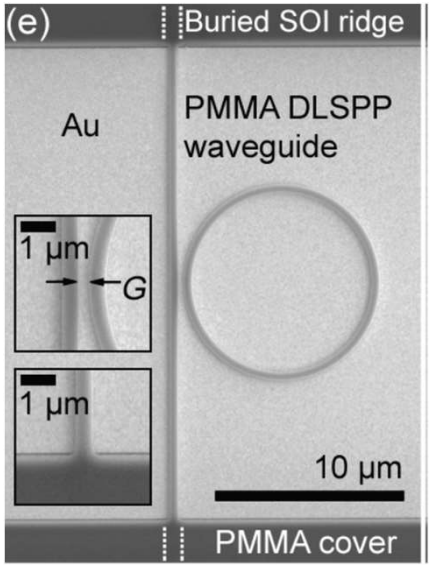

A. Dereux, *et al.*, *Proceedings of SPIE*, 7945, 2011

Introduction: The Big Picture & Challenges

Contrary to passive DLSPP components, switching elements are still in their infancy. If successful, DLSPP switches can be used as the core element of high-throughput routers in a hybrid Silicon-Plasmonic technology.

Layout of a 2x2 router architecture based on merging Plasmonics with Silicon Photonics.

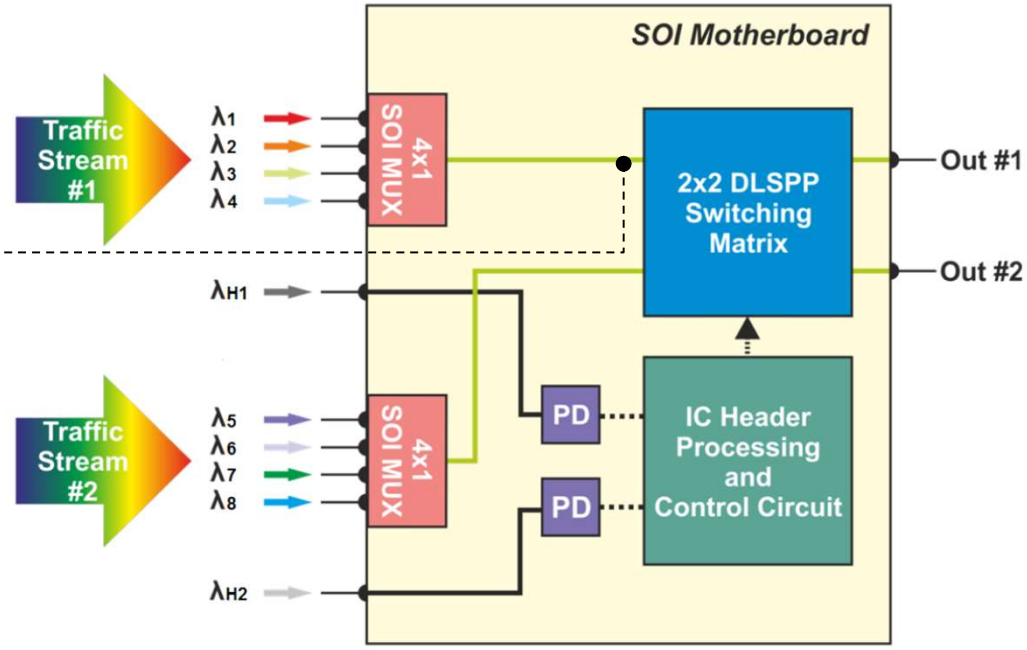

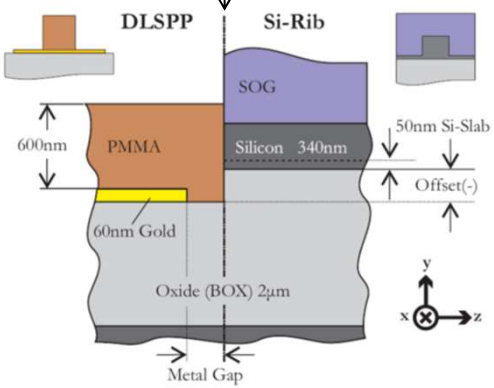

Low-loss interface between the DLSPP & Si guide.

S. Papaioannou, *et al.*, *sub. to J. Lightwave Technol.*, 2011

Introduction: The Big Picture & Challenges

Current plasmonic switching elements have poor performance, mainly due to the inherent losses. The challenge is to meet the performance anticipated in real-world optical interconnect applications:

- High Extinction Ratio (ER), >10 dB
- Tolerable Insertion Losses (IL), <10 dB
- Bandwidth to accommodate few 100-GHz-spaced WDM channels, >6 nm
- Acceptable switching speed, 1 μs

We will show that we can design plasmonic switching elements that can meet these targets!

Two approaches:

- **Resonant** Elements based on DLSPP microrings.
- **Longitudinal** Elements following an MMI layout.

Outline

- Introduction
  - The DLSPP Waveguide
  - DLSPP-Based Components
  - The Big Picture & Challenges
- Microring-Based Resonant Switching Elements
  - Classic Add-Drop Filter
  - 3D FEM Implementation Details
  - Waveguide Crossing
  - Add-Drop Filter with Perpendicular Access Waveguides
  - Dual-Resonator Add-Drop filter with perpendicular access waveguides
- Longitudinal Switching Elements
  - A Multi-Mode Interference (MMI) Approach
  - 3D BPM Implementation Details
  - Dispersion Studies
  - Theoretical Bounds in Performance
  - Switch Evaluation using BPM
- Conclusions

Microring-Based Resonant Switching Elements

A family of microring based DLSPP elements:

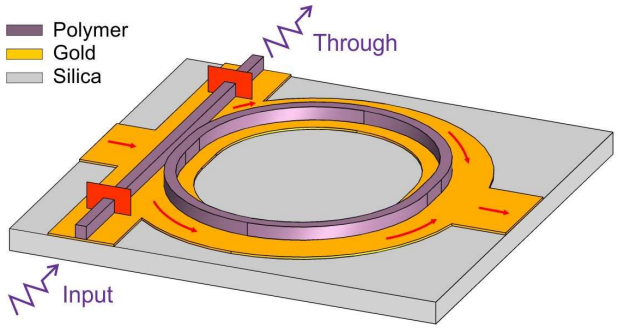

I. All-pass filter

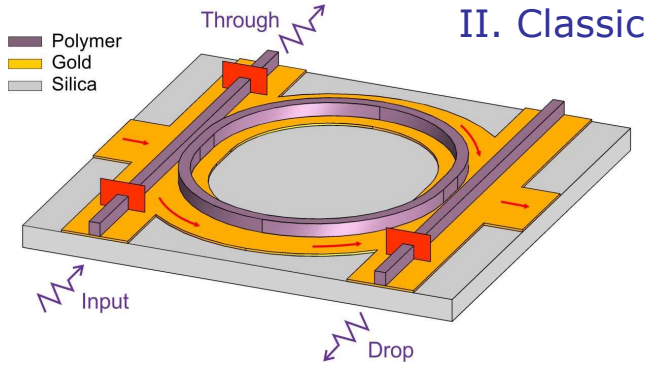

II. Classic Add-Drop

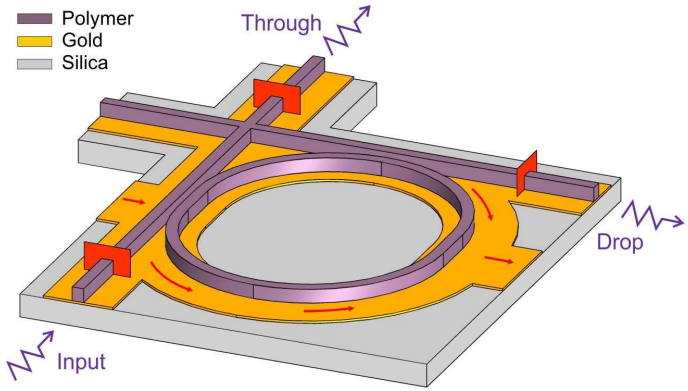

III. Add-Drop with perpendicular access guides

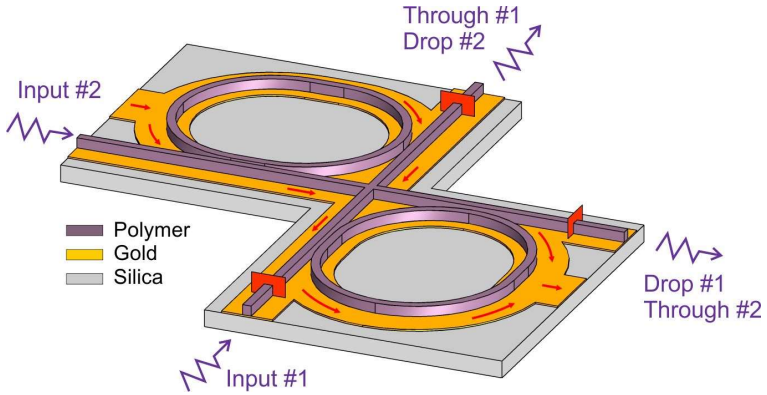

IV. Dual-resonator Add-Drop with perpendicular access guides

Classic Add-Drop Filter

- Racetracks to increase coupling
- Asymmetric gaps g_1 & g_2 for optimized 1x2 operation
- Asymmetric metal placement (w_{Au}=3 μm)
- R~5 μm: compromise between resistive & bending losses

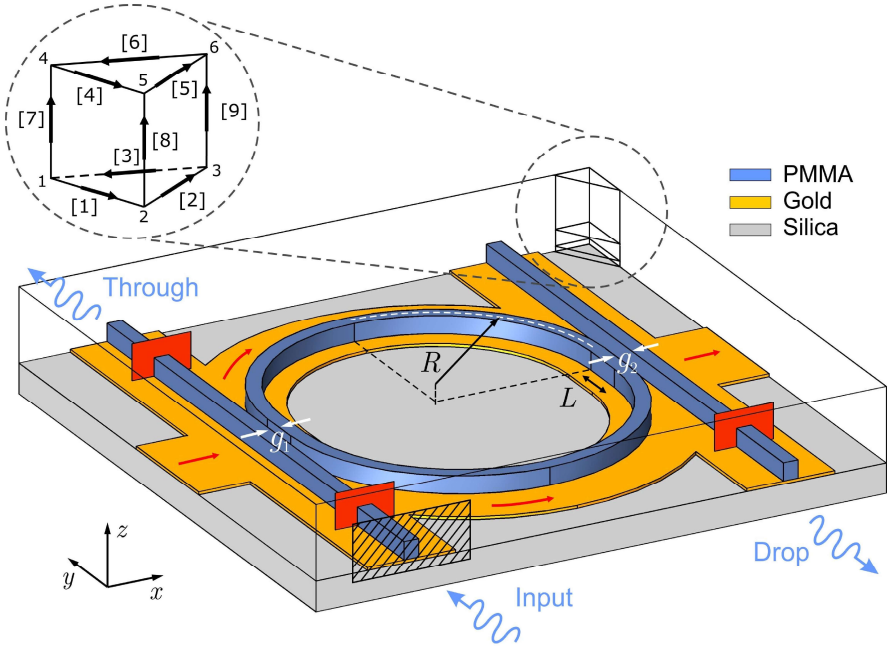

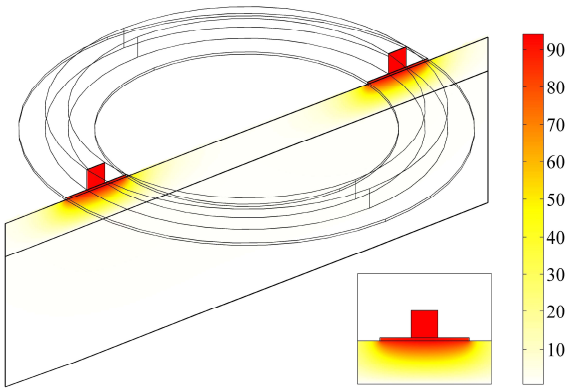

O. Tsilipakos, *et al.*, *J. Appl. Phys.*, *109*, *073111*, 2011

O. Tsilipakos, *et al.*, *J. Appl. Phys.*, *106*, *093109*, 2009

Injecting current in the gold → the polymer is heated → the refractive index is changed by the thermo-optic effect → the resonance frequency is shifted.

Classic Add-Drop Filter

TOC = -2.9×10^{-4} K^{-1}, n_p = 1.52 @ 25 °C
ΔT = 100 K → TO shift = 25 nm

- Complete variation captured (FSR/2)
- Not TOC-limited (ER_{drop} = ER_{ideal} = ~6 dB)
- Architecture-limited
- Absence of interference for drop port
- ER_{drop} ↑ if g_2 ↑ but then IL_{drop} ↑
- Even poorer performance for 2x2 operation

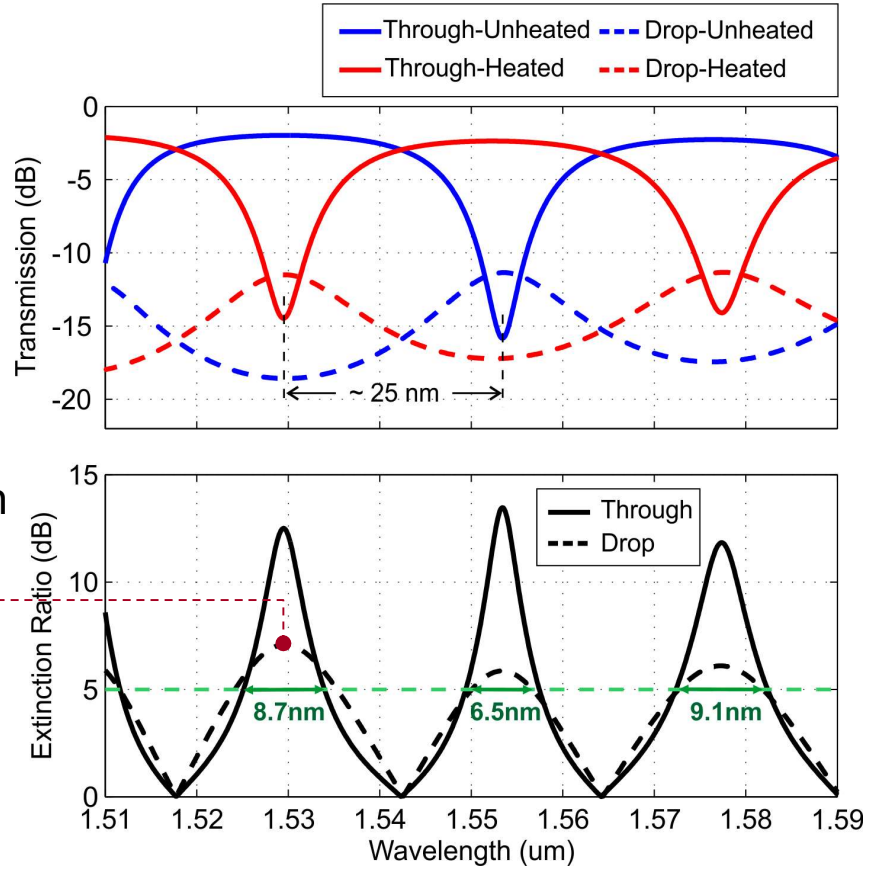

Poor drop port performance!

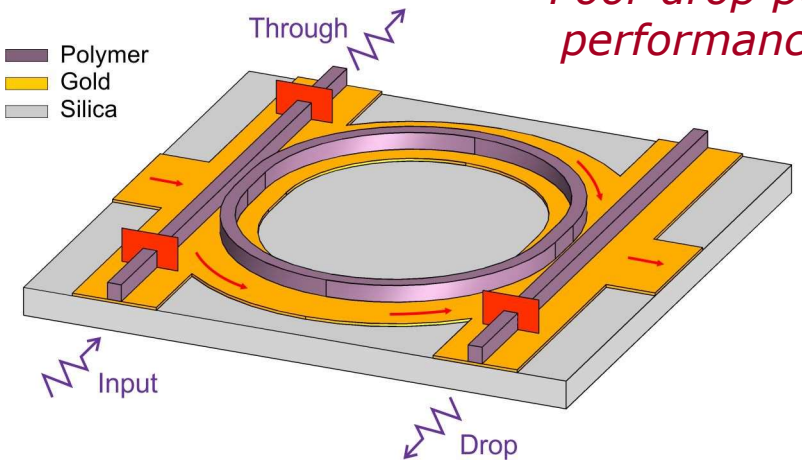

R = 5.2, L = 0.5, g_1 = 0.3, g_2 = 0.6 μm

3D FEM Implementation Details

✓ 1st order triangular prisms
- 10 prism layers → 1(SiO_2)+2(Au)+4(Pol.)+3(Air)

✓ 1st order absorbing boundary conditions (ABCs) on all sides of the bounding box.

$$\hat{\mathbf{n}} \times (\nabla \times \mathbf{E}) + jk_0 \hat{\mathbf{n}} \times (\hat{\mathbf{n}} \times \mathbf{E}) = 0$$

✓ Modified B/C for the excitation & absorption of hybrid modes in waveguide ports.

$$\hat{\mathbf{n}} \times \nabla \times \mathbf{E} + \bar{\bar{\gamma}} \hat{\mathbf{n}} \times \hat{\mathbf{n}} \times \mathbf{E} = 2\bar{\bar{\gamma}} \hat{\mathbf{n}} \times \hat{\mathbf{n}} \times \mathbf{E}^{\mathrm{inc}}$$

$$\bar{\bar{\gamma}} = \frac{j\omega\mu_0}{Z_w^{\mathrm{TE}}(u,v)} \hat{\mathbf{u}}\hat{\mathbf{u}} + \frac{j\omega\mu_0}{Z_w^{\mathrm{TM}}(u,v)} \hat{\mathbf{v}}\hat{\mathbf{v}}.$$

Correct **tensorial** representation for a hybrid mode

$$Z_w^{\mathrm{TE}}(u,v) = \frac{E_u(u,v)}{H_v(u,v)}, \qquad Z_w^{\mathrm{TM}} = -\frac{E_v(u,v)}{H_u(u,v)}.$$

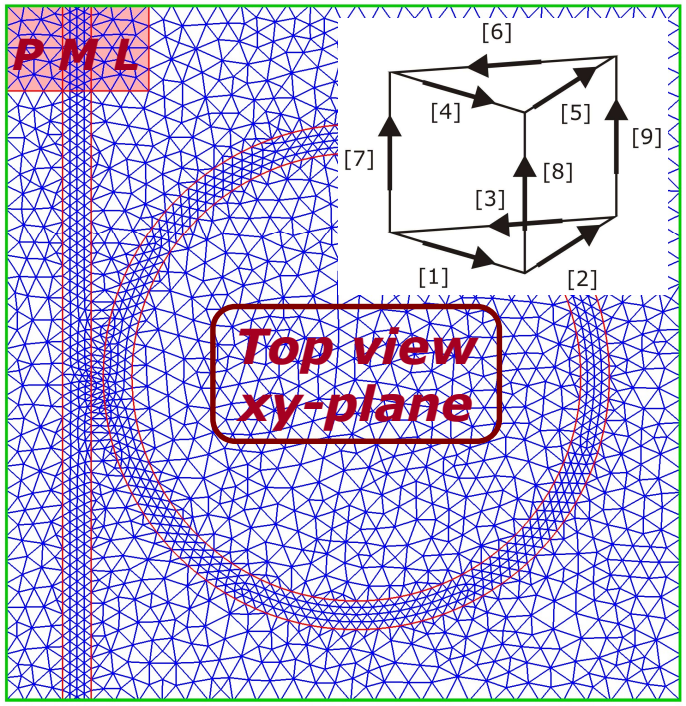

✓ Perfectly matched layer (PML) for the reflectionless termination of the bus w/g.
- Only **locally** employed. Global utilization would increase DoFs & degrade conditioning.

Waveguide Crossing

Untreated DLSPP Waveguide Crossing

- IL ~ 0.5 dB
- Diffraction in crossing
- Reflection from crossing
- Coupling to perpendicular w/g's (XT)
- XT ~ -15 dB. Not negligible! Normalized amplitude of the cross-coupled field ~ 0.2.

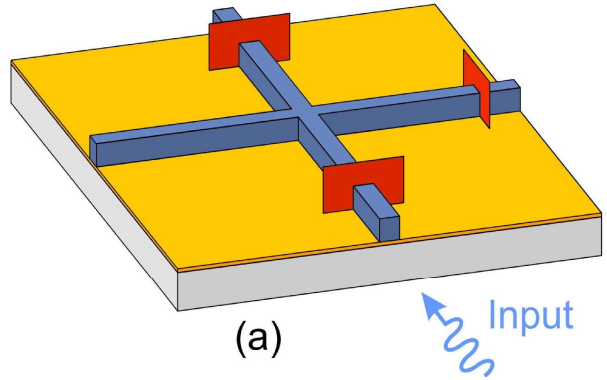

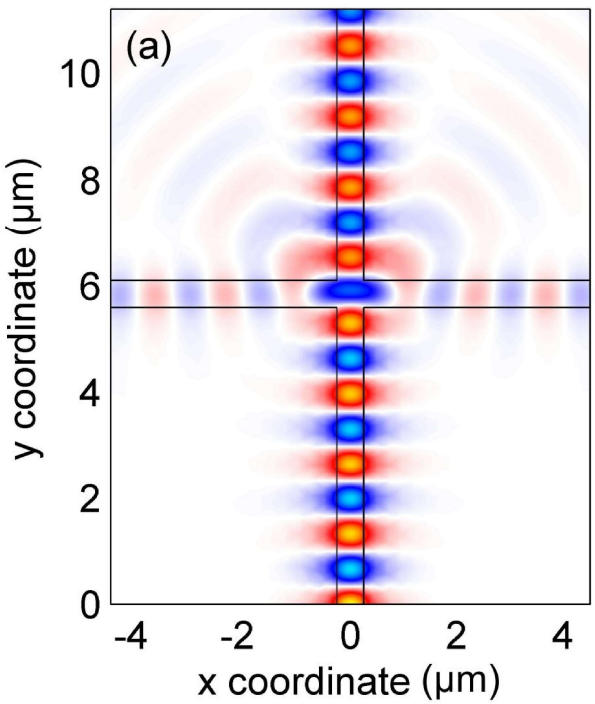

In Silicon Photonics

- IL > 1 dB
- XT ~ -9 dB

Worse performance due to stronger mode confinement.

W. Bogaerts *et al.*, *Opt. Lett.*, **32**, 2801, 2007

Waveguide Crossing

Key idea to suppressing the XT: the mode confinement is relaxed just before it arrives at the waveguide intersection. This is done by some kind of tapering that expands the guided mode.

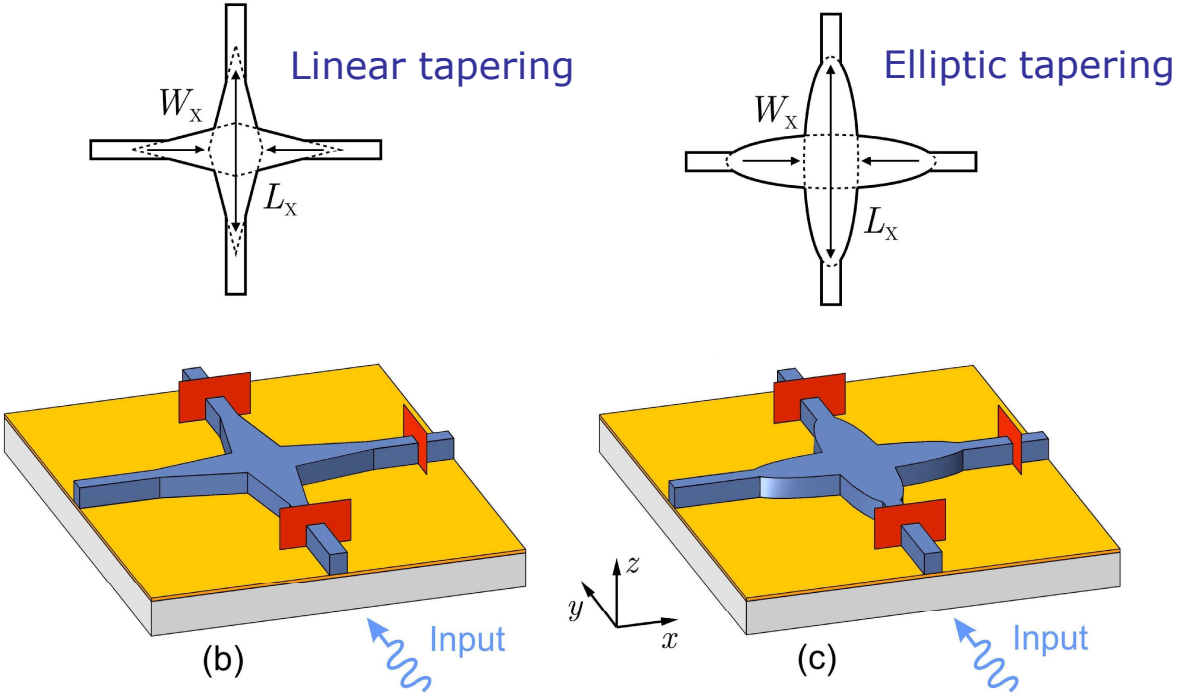

Treated DLSPPW Crossing

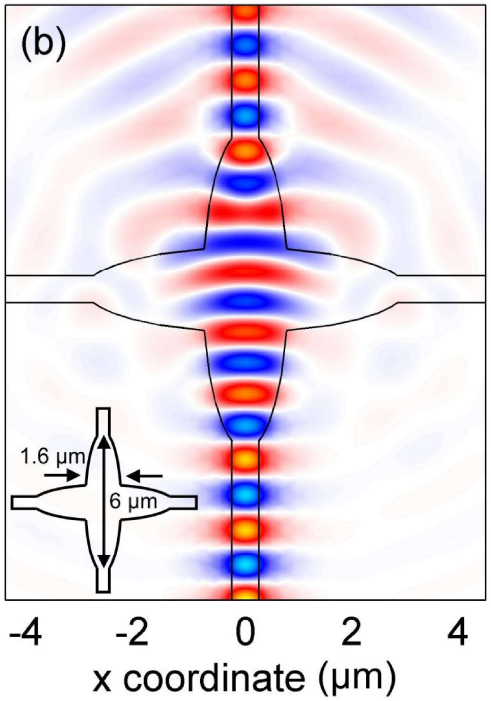

Waveguide Crossing

- Crosstalk is suppressed to -35dB.
- IL slightly increased at ~-0.8 dB.
- Negligible reflection.
- Almost negligible spectral variation (~0.2 dB in C-band).
- Elliptical tapering superior to linear.

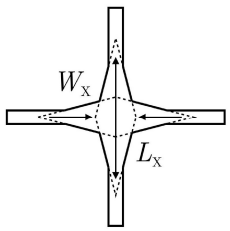

Linear tapering

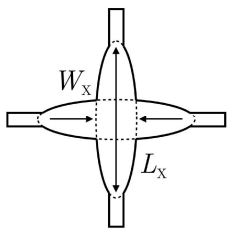

Elliptic tapering

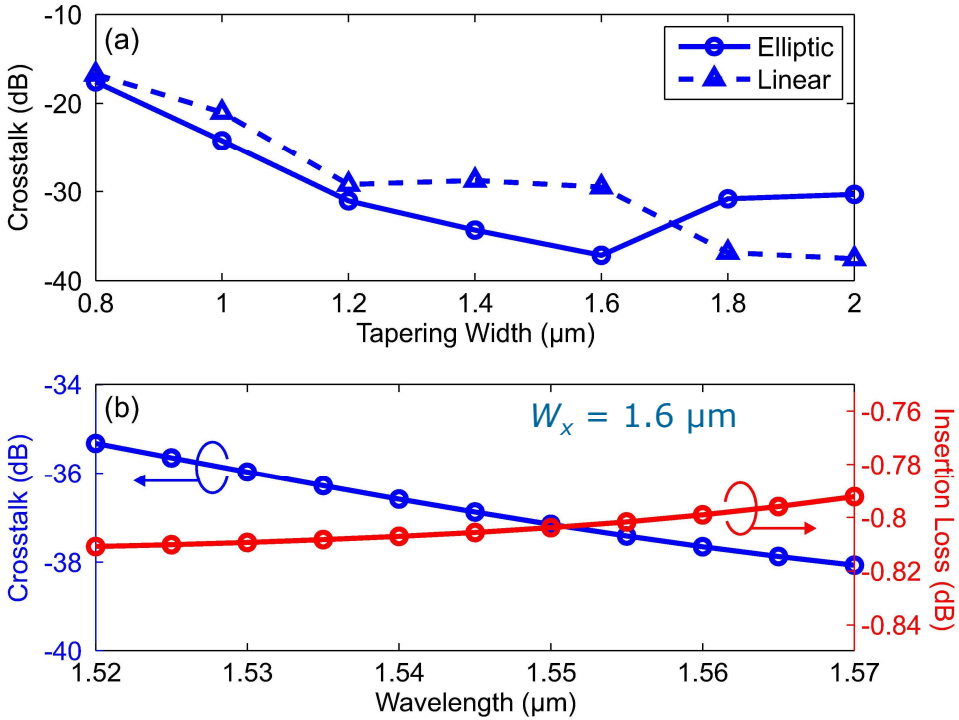

L_x = 6 μm

Add-Drop Filter with Perpendicular Access Waveguides

Can we improve the performance by perpendicular access guides?

Key idea: provide a destructive interference mechanism that will lower the drop port transmission minima → improvement in ER!

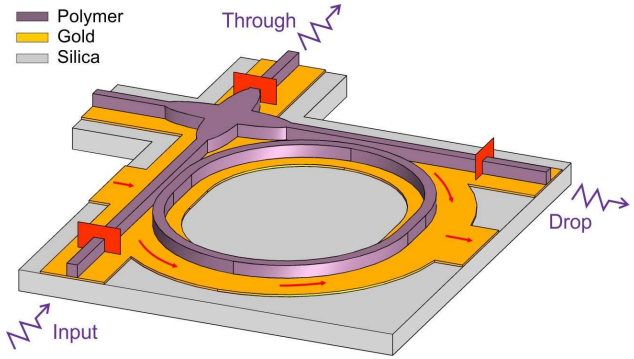

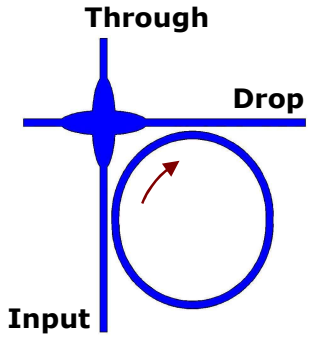

Treated WGX

- As classic Add-Drop with different orientation of drop port.
- ER of drop port does not improve.
- IL of drop only slightly improves.

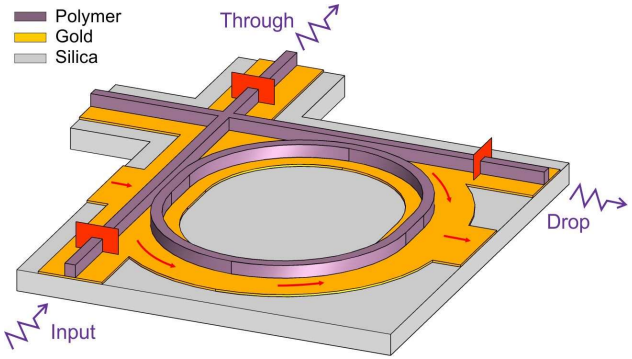

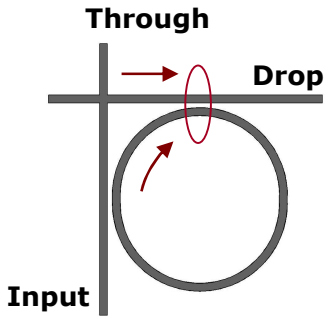

UnTreated WGX

- Transmission of drop port a result of **interference.**
- **ER of drop can improve!**
- max(drop) ≠ min(thru)

However, symmetry is broken and thus cannot be used as a 2x2 switch!

Add-Drop Filter with Perpendicular Access Waveguides

- Interference effects reshape the drop port transmission; steeper segments appear.
- Maxima & minima no longer coincide.
- Can only act as a 1x2 switch.

ER > 10 dB for both ports over 3.5 nm
IL_{drop} ~10 dB

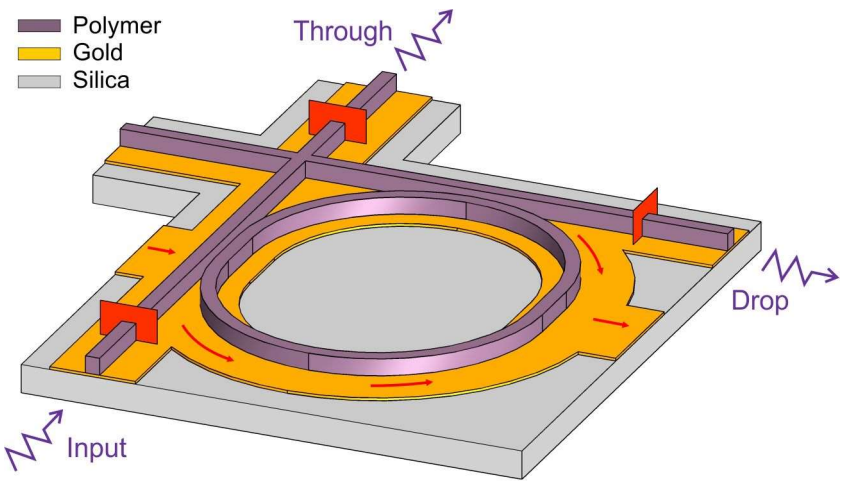

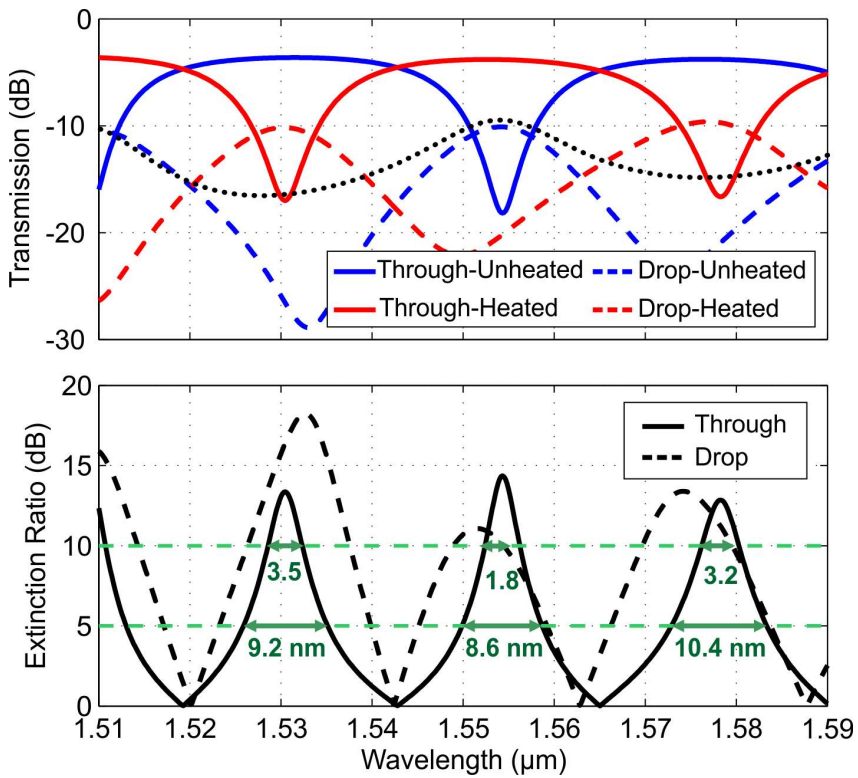

$R = 5.2$, $L = 0.5$, $g_1 = 0.3$, $g_2 = 0.5$ μm

Dual-Resonator Add-Drop filter with perp. access guides

- Restores symmetry → 2x2 switches are possible.
- New route for interference through the second ring (Q-route), though not as strong as the WGX crosstalk, especially since g_2 is large.

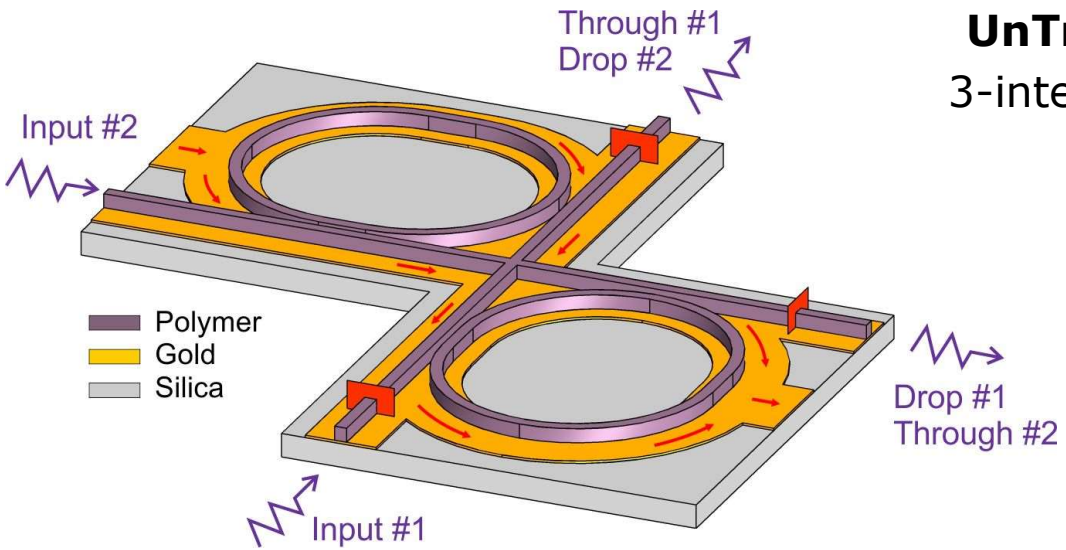

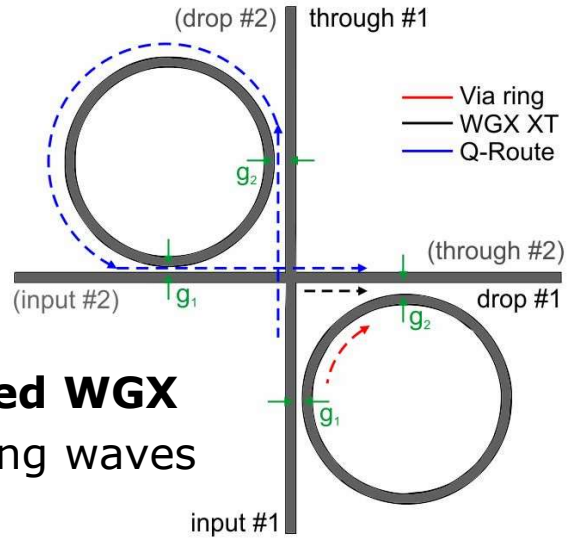

UnTreated WGX
3-interfering waves

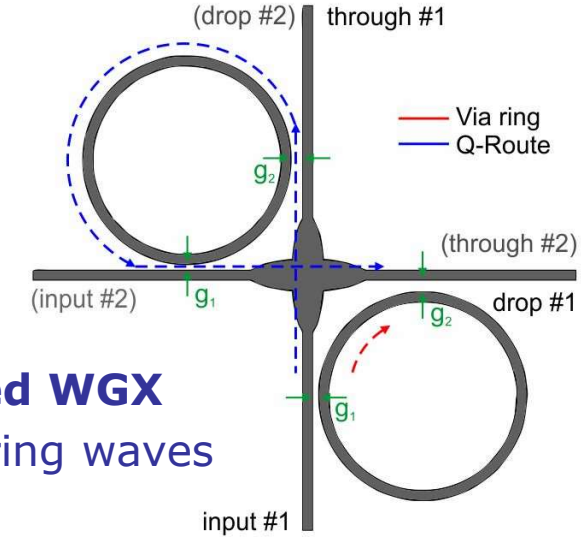

Treated WGX
2-interfering waves

Dual-Resonator Add-Drop filter with perp. access guides

- Irregular shape in drop port due to interference effects.
- Max ΔT does not guarantee optimum; depends on curve shape.
- ΔT=55 K (T_{max}=80 °C): $\Delta\lambda_{TO}$=13 nm

  ER > 10 dB for both ports over 4.5 nm

  IL_{drop} < 10 dB

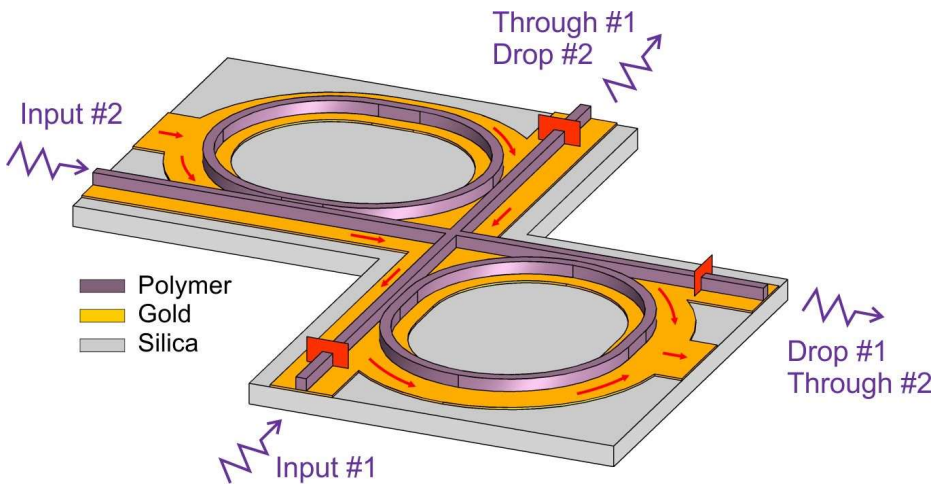

ΔT = 55 K ⇒ $\Delta\lambda_{TO}$ ~ 13 nm

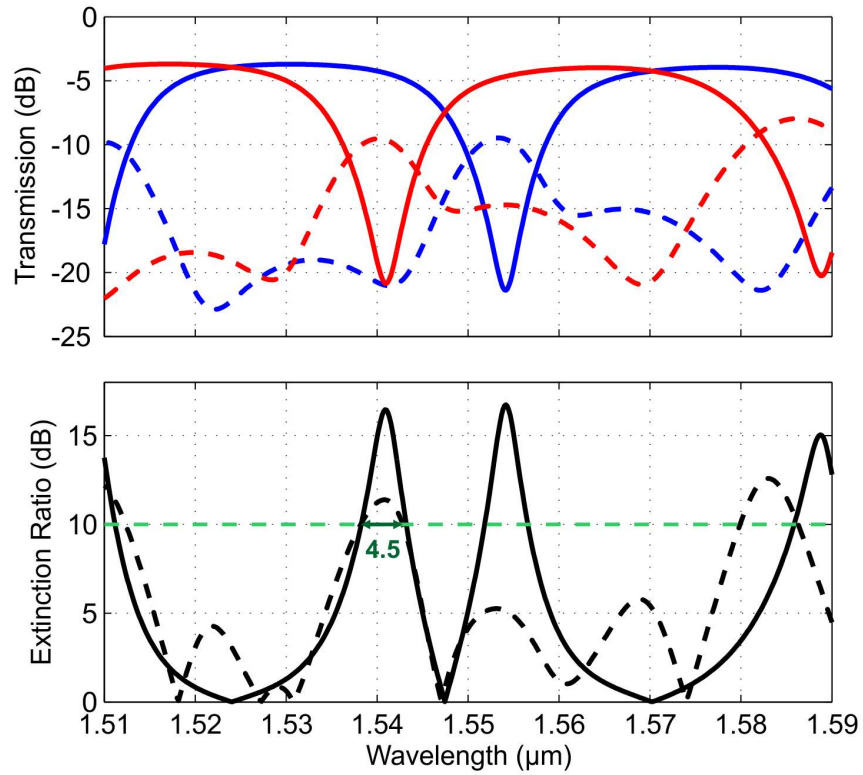

R = 5.2, L = 0.5, g_1 = 0.3, g_2 = 0.5 μm

Outline

- Introduction
  - The DLSPP Waveguide
  - DLSPP-Based Components
  - The Big Picture & Challenges
- Microring-Based Resonant Switching Elements
  - Classic Add-Drop Filter
  - 3D FEM Implementation Details
  - Waveguide Crossing
  - Add-Drop Filter with Perpendicular Access Waveguides
  - Dual-Resonator Add-Drop filter with perpendicular access waveguides
- Longitudinal Switching Elements
  - A Multi-Mode Interference (MMI) Approach
  - 3D BPM Implementation Details
  - Dispersion Studies
  - Theoretical Bounds in Performance
  - Switch Evaluation using BPM
- Conclusions

Longitudinal Switching Elements

Exploit mode interference in a longitudinal arrangement:

- Less compact compared to resonant (micro-ring) elements.
- Improvement in B/W expected.
- Almost equivalent performance (IL, ER & XT) for both ports.

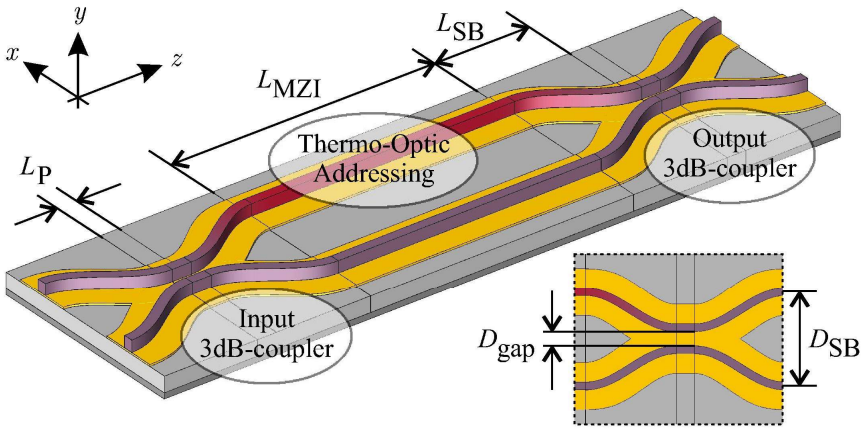

Mach-Zehnder Interferometer layout

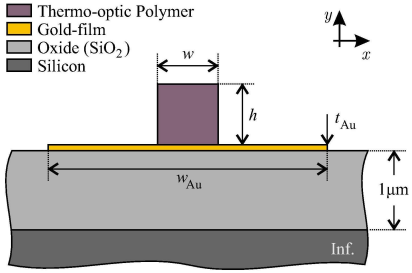

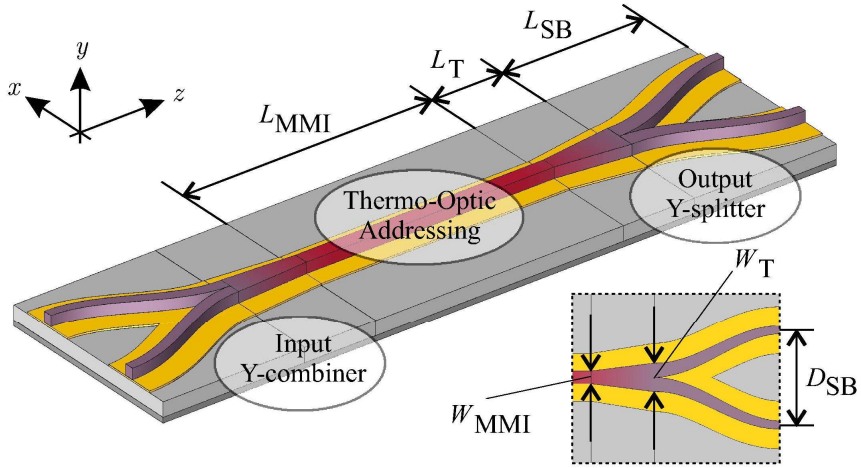

Multi-Mode Interference layout

A Multi-Mode Interference (MMI) Approach

- The MMI section supports the fundamental (symmetric) and only one higher order (*anti-symmetric*) mode.
- The two modes interfere with a beating length L_B.
- Beating length is slightly different when MMI section is in the **Heated** or **Unheated** state.
- For the appropriate MMI length a phase-difference of π is accumulated.

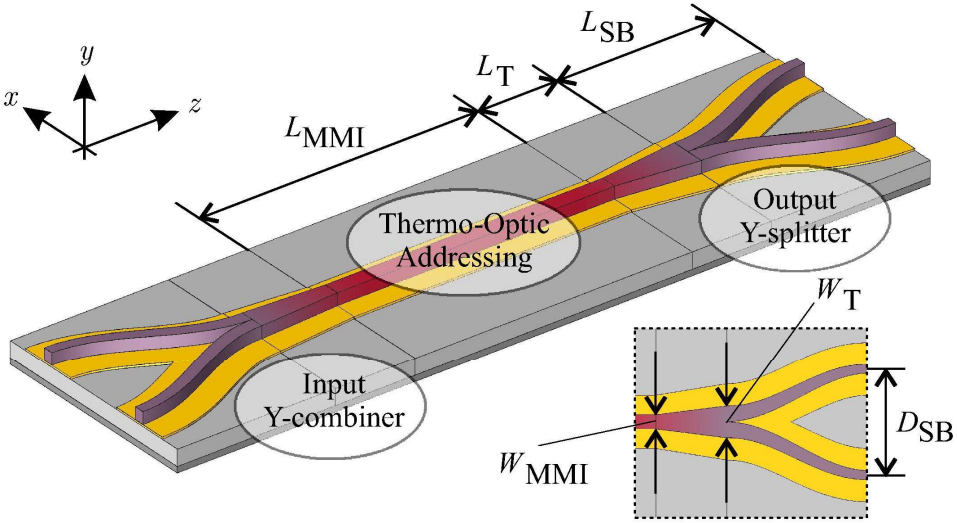

$$L_B = \frac{\lambda_0 / 2}{\Delta n_{\text{eff}}^{\text{S-A}}}, \quad \Delta n_{\text{eff}}^{S\text{-}A} \equiv n_{\text{eff}}^{S} - n_{\text{eff}}^{A}$$

A difference in the beating lengths of the **Heated** and **Unheated** states is translated, after sufficient MMI length, to a phase-difference of π, so that the output ports are exchanged.

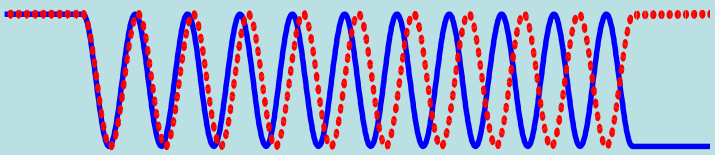

3D BPM Implementation Details

✓ Full-Vector Beam Propagation Method based on Finite-Elements

- Mixed element: Edge elements for transverse E + Nodal elements for E_z

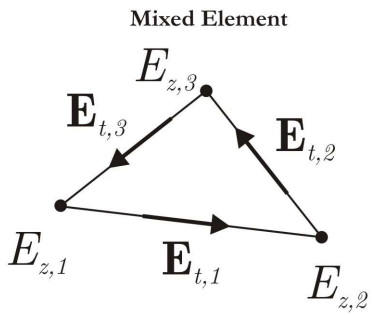

✓ Transverse & axial components coupled: CN scheme

$$[A]\frac{\partial^2 \tilde{\mathbf{E}}'}{\partial z^2} - 2jk_{\mathrm{ref}}[B]\frac{\partial \tilde{\mathbf{E}}'}{\partial z} + [C]\tilde{\mathbf{E}}' = \mathbf{0} \qquad \mathbf{E}' = [\mathbf{E}_t, E_z']^T$$

K. Saitoh and M. Koshiba, *J. Lightwave. Technol., 19, 405,* 2001

$$[A] \equiv [B] = \begin{bmatrix} M_{tt} & -L_{tz} \\ -L_{zt} & -K_{zz} \end{bmatrix}, [C] = \begin{bmatrix} K_{tt} - k_{\mathrm{ref}}^2 M_{tt} & k_{\mathrm{ref}}^2 L_{tz} \\ k_{\mathrm{ref}}^2 L_{zt} & k_{\mathrm{ref}}^2 K_{zz} \end{bmatrix}$$

O. Tsilipakos *et al.*, *Opt. Quantum Electron.*, 2011

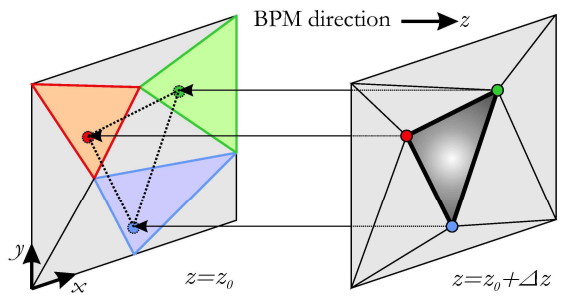

✓ FE-mesh transformations for z-dependent structures.

✓ Wide-Angle corrections according to the multi-step algorithm by Hadley.

✓ Perfectly matched layer (PML) for the termination of the transverse window.

Dispersion Studies

- We restrict our attention to the two-mode interference regime: beating modes are TM_{00} & TE_{00}.
- TE_{00} is similar to TM_{10} w.r.t. E_y.
- TE_{00} suffers much lower losses compared to TM_{00}.
- Also, the differential losses between TM_{00}-TE_{00} are different in **Heated (H)** & **Unheated (U)** states.
- We adopt w_{MMI} = 800 nm as a fair compromise. (L_{MMI} kept short).

h = 600 nm, gold film = 3 μm x 100 nm,
ΔT = 100 K, TOC = -3x10^{-4} K^{-1}

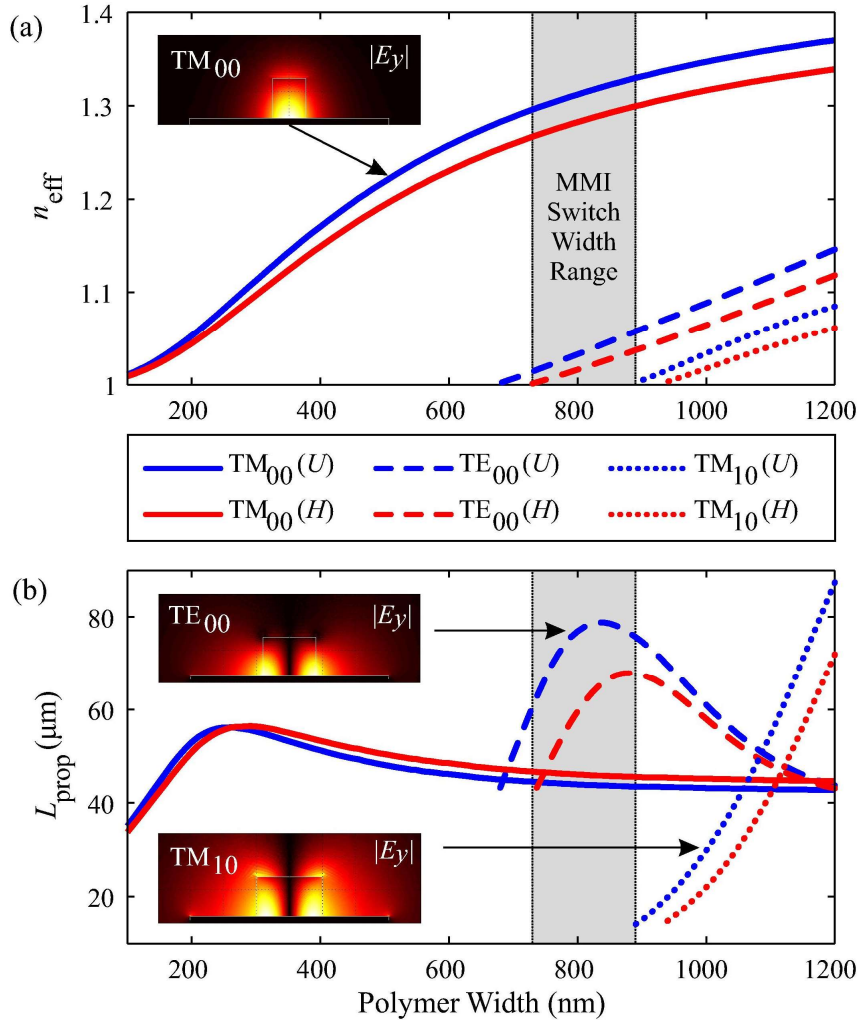

Theoretical Bounds in Performance

Before employing any heavy BPM simulations, we will assess the theoretical bounds in performance using a simple analytical model: no substitute for robust numerical modeling but very useful & insightful.

Field at output ports 1&2 as an interference of the two modes.

$$E_{1,2}(z) = E_S(z) \pm E_A(z) = \sqrt{R_{S/A}}\, e^{-\gamma_S z} \pm e^{-\gamma_A z}$$

Power excitation ratio by input Y-junction

Eigenvalue analysis input for **U** & **H** states:

$$\gamma_q = \frac{1}{2L_{\text{prop}}} + j\frac{2\pi}{\lambda} n_{\text{eff}},$$

$$q = \{S, A\} \equiv \{\text{TM}_{00}, \text{TE}_{00}\}$$

Output-Port Extinction Ratio

$$\text{ER}(z) \triangleq |E_1(z)|^2 / |E_2(z)|^2 \longrightarrow \text{ER}_{\min} = \min\left\{\left|\text{ER}_{(H)}\right|, \left|\text{ER}_{(U)}\right|\right\}$$

Phase-match length

$$L_{\text{MMI}} = \frac{L_{B(U)} L_{B(H)}}{\left|L_{B(U)} - L_{B(H)}\right|} = \frac{\lambda_0 / 2}{\left|\Delta n_{\text{eff,(U)}}^{\text{S-A}} - \Delta n_{\text{eff,(H)}}^{\text{S-A}}\right|}$$

Upper Bound #1

$$\text{ER}_{\Delta\phi}(z) = \tan^2\left[\frac{\pi}{4}\left(\frac{z}{L_{\text{MMI}}} + 1\right)\right]$$

Envelope of $\text{ER}_{\min}$ for an MMI waveguide of length z

Theoretical Bounds in Performance

Characteristic length for measuring the propagation-length difference between S & A modes.

$$L_{\Delta\alpha} \triangleq 4\frac{L_{\text{prop}}^{\text{S}} L_{\text{prop}}^{\text{A}}}{\left|L_{\text{prop}}^{\text{S}} - L_{\text{prop}}^{\text{A}}\right|}$$

(different for **U** & **H** states)

Upper Bound(s) #2

$$\text{ER}_{\Delta\alpha}(z) = \coth^2\left(\frac{z}{L_{\Delta\alpha}} - \frac{\ln(R_{S/A})}{4}\right)$$

Limitation in ER due to the L_{prop} difference between S & A modes. (different for **U** & **H** states)

Optimal value for the power excitation ratio:

$$R_{S/A} = \exp\left[2L_{\text{MMI}}\left(\frac{1}{L_{\Delta\alpha},(U)} + \frac{1}{L_{\Delta\alpha},(H)}\right)\right]$$

$$L_{\Delta^2\alpha} \triangleq 2\frac{L_{\Delta\alpha,(U)} L_{\Delta\alpha,(H)}}{\left|L_{\Delta\alpha,(U)} - L_{\Delta\alpha,(H)}\right|}$$

The difference of the characteristic lengths $L_{\Delta\alpha}$ for states **U** & **H** also limits ER.

Max. theoretic ER predicted by model using eigenmode analysis input (when $R_{S/A}$ is optimized)

Upper Bound #3

$$\text{ER}_{\max} = \coth^2\left(\frac{L_{\text{MMI}}}{L_{\Delta^2\alpha}}\right)$$

Theoretical Bounds in Performance

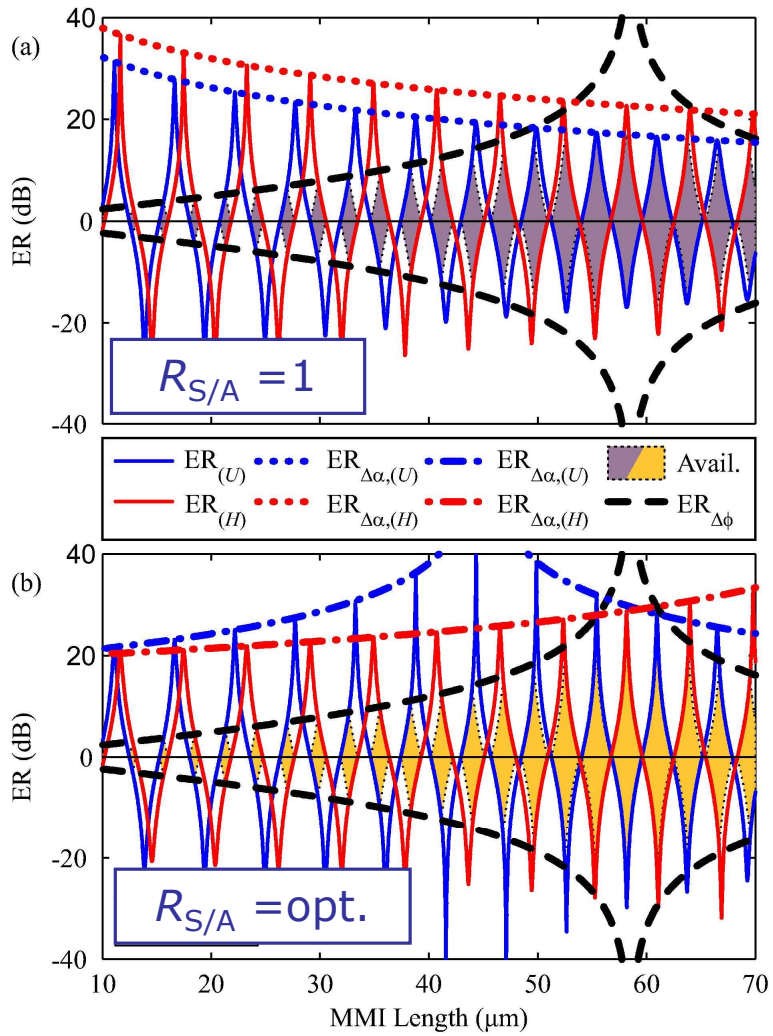

ER evolution along the MMI waveguide and limiting bounds #1, #2 & #3.

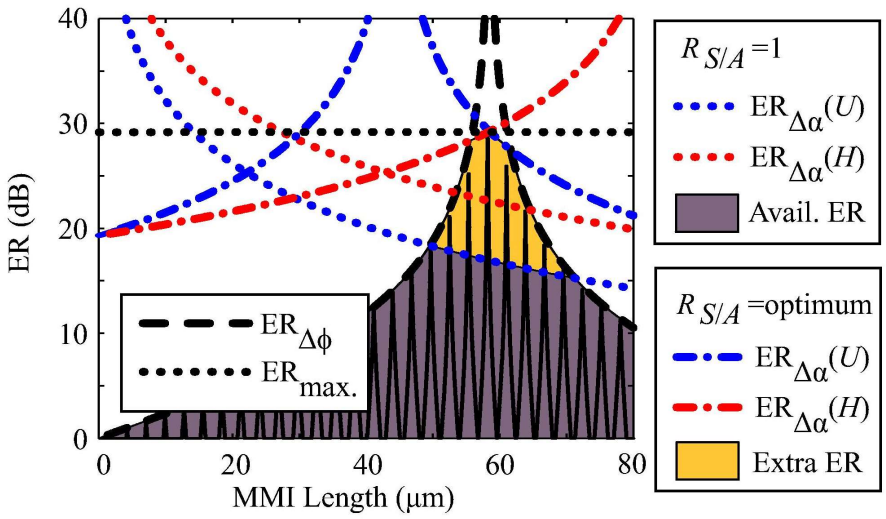

A 10dB improvement is possible for optimum $R_{S/A}$.

Switch Evaluation using BPM

The input and output Y-junctions are designed to provide the optimum $R_{S/A}$ excitation ratios with the FV-BPM.

$$R^{\text{in}}_{S/A} = 1.55$$

$$R^{\text{out}}_{S/A} = 1.0$$

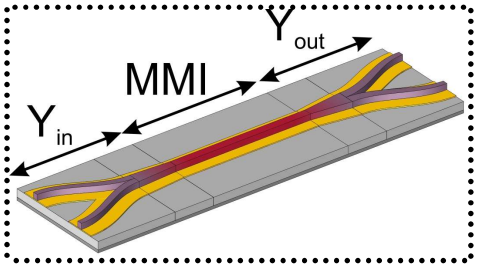

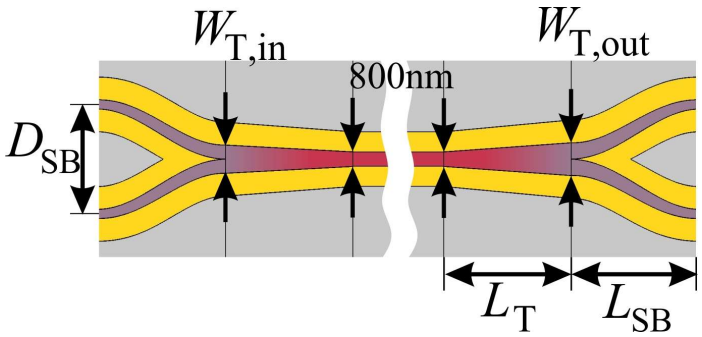

$D_{SB} = 6$, $L_{SB} = 10$, $L_T = 10$,

$W_{T,\text{in}} = 1.05$, $W_{T,\text{out}} = 1.3$ μm

FE-BPM calculated ER vs. MMI guide length for the entire component: Y_{in} + MMI + Y_{out}

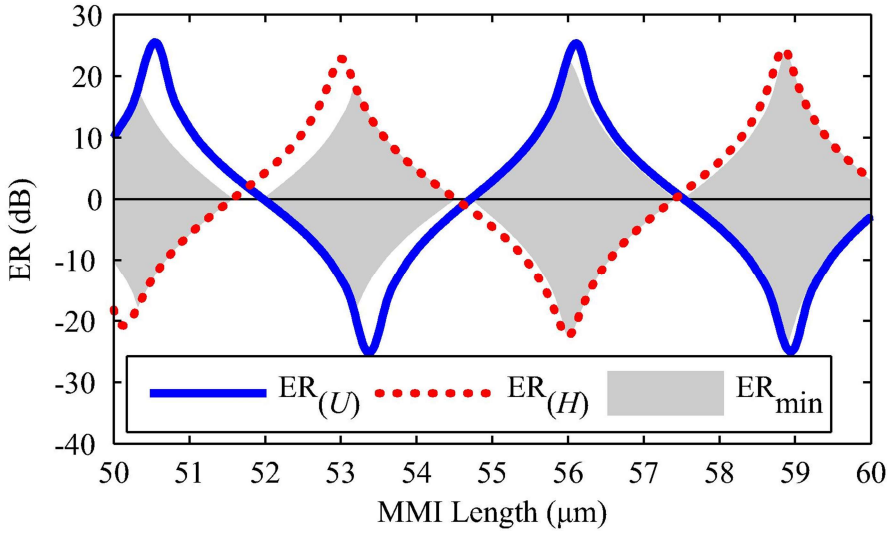

FE-BPM
Max ER_{min} ~24 dB at 58.9 um

Analytical Eigenmode-based model
Max ER_{min} ~29 dB at 58.2 um

Switch Evaluation using BPM

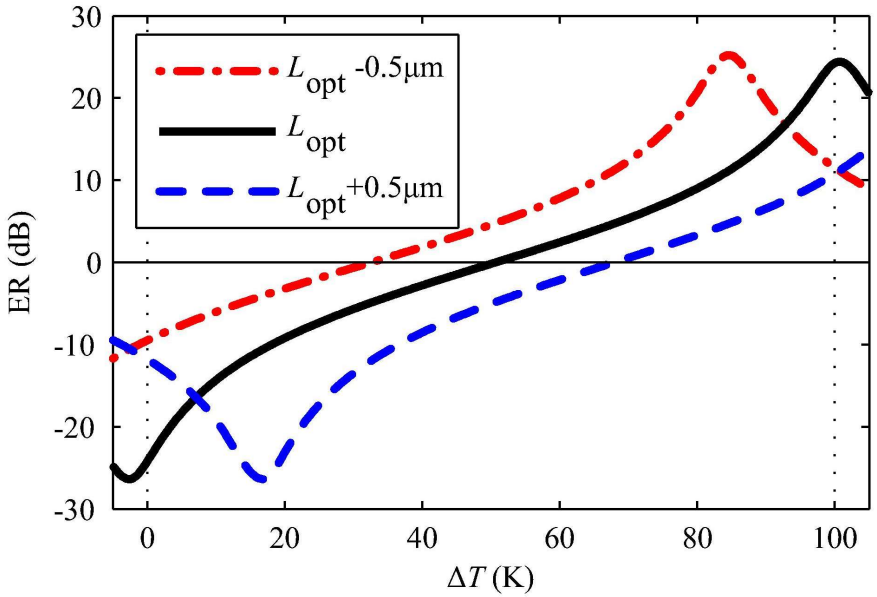

FE-BPM calculated ER vs. Δ*T* for the entire component: Y_{in} + MMI + Y_{out}

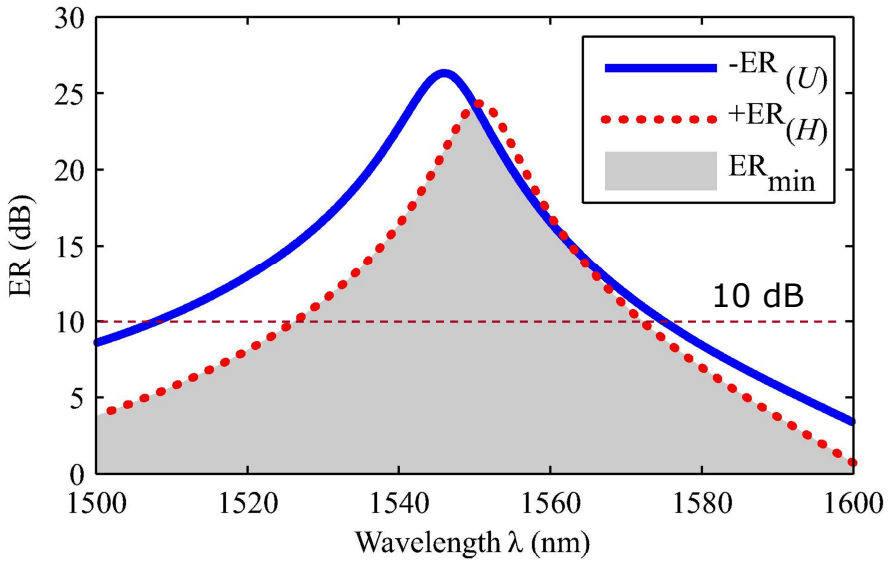

FE-BPM calculated ER vs. λ for the entire component: Y_{in} + MMI + Y_{out}

- Small deviations from the optimum MMI length lead to ER degradation in one of the switch-states.
- The other can always be compensated by changing *T*.

- ER_{min} > 10 dB for a 45 nm bandwidth.
- 25nm shift for a 0.5um shift from the optimum MMI length.

Outline

- Introduction
  - The DLSPP Waveguide
  - DLSPP-Based Components
  - The Big Picture & Challenges
- Microring-Based Resonant Switching Elements
  - Classic Add-Drop Filter
  - 3D FEM Implementation Details
  - Waveguide Crossing
  - Add-Drop Filter with Perpendicular Access Waveguides
  - Dual-Resonator Add-Drop filter with perpendicular access waveguides
- Longitudinal Switching Elements
  - A Multi-Mode Interference (MMI) Approach
  - 3D BPM Implementation Details
  - Dispersion Studies
  - Theoretical Bounds in Performance
  - Switch Evaluation using BPM
- Conclusions

Conclusions

Our studies reveal that it is possible to design DLSPP switching elements that can meet the requirements of practical interconnect applications for loading materials with a TOC of $-3x10^{-4}$ K^{-1}.

- **Microring-based Elements**
  - ER > 10 dB for both ports and over 4 nm B/W
  - IL_{drop} < 10 dB and $IL_{through}$ ~5 dB
  - Footprint ~20x20 um^2
- **Longitudinal (MMI)-based Elements**
  - Best ER ~25 dB, with ER > 10 dB over 45 nm B/W
  - IL ~11 dB for both ports
  - Footprint ~100x10 um^2
- Switching speed can be ~ 2 μs if the component resides on a SOI wafer.

This work was supported in part by the European FP7 project **PLATON** [Contract No. 249135]

http://www.ict-platon.eu